Thin Solid Films 553 (2014) 109–113

Contents lists available at ScienceDirect

Thin Solid Films

journal homepage: www.elsevier.com/locate/tsf

Study of ferroelectric/dielectric multilayers for tunable stub resonator applications at microwaves

Y. Corredores [a], A. Le Febvrier [b], X. Castel [a,*], R. Sauleau [a], R. Benzerga [a], S. Députier [b], M. Guilloux-Viry [b], A. Mekadmini [c], N. Martin [c], G. Tanné [c]

[a] IETR, UMR-CNRS 6164, IUT de Saint-Brieuc, Université de Rennes 1, 18 rue Henri Wallon, 22004 Saint-Brieuc et 263 avenue du Général Leclerc, 35042 Rennes, France
[b] ISCR, UMR-CNRS 6226, Université de Rennes 1, 263 Avenue du Général Leclerc, 35042 Rennes, France
[c] Lab-STICC, UMR-CNRS 6285, Université de Bretagne Occidentale, 6 Avenue Le Gorgeu, 29238 Brest, France

ARTICLE INFO

Available online 20 November 2013

Keywords:
Dielectric/ferroelectric heterostructure
Multilayer
Dielectric film
Ferroelectric film
Tunable resonator
Microwave

ABSTRACT

Tunable coplanar waveguide stub resonators deposited on various ferroelectric/dielectric heterostructures are studied in the 10-GHz band. A frequency tunability of up to ~45% is achieved under a moderate biasing field (E_{bias} < 100 kV/cm) when the resonator is printed on $KTa_{0.5}Nb_{0.5}O_3$ (KTN) ferroelectric thin film alone: this comes from the large permittivity agility of the KTN material ($\varepsilon_{r(KTN)}$ varies from ~700 to ~200). Nevertheless this also leads to significant insertion loss due to the dielectric loss of the ferroelectric material itself ($\tan\delta_{r(KTN)} \approx 0.15$–0.30 at 10 GHz). In this paper, an original route has been considered to reduce the device loss while keeping up a high frequency tunability. It consists in associating the KTN film with a dielectric film to elaborate ferroelectric/dielectric multilayers. The $Bi_{1.5}Zn_{0.9}Nb_{1.5}O_{7-\delta}$ (BZN) oxide material is selected here for two main reasons, namely its low dielectric loss ($\tan\delta_{r(BZN)} \approx 0.005$–0.0075) and its moderate relative permittivity ($\varepsilon_{r(BZN)} \approx 95$–125) at 12.5 GHz. The relevance of this approach is studied numerically and experimentally. We compare numerically two different heterostructures for which the ferroelectric film is grown on the dielectric film (KTN/BZN), or vice versa (BZN/KTN). A stub resonator printed on the most relevant heterostructure has been fabricated, and experimental data are discussed and compared to the numerical results.

1. Introduction

Nowadays numerous wireless applications require advanced miniature and adaptive components or devices at microwaves, e.g. [1–4], especially to cope with the wide diversity of available communication standards. In particular reconfigurable filters, resonators and antennas, e.g. [5–7] are key building blocks of future radio front-ends. In this frame, ferroelectric oxides are promising candidates to design such devices [8–10] as their large relative permittivity ensures circuit miniaturization and is also controlled by an external static electric field (E_{bias}). Moreover their deposition in thin films offers the ability to fabricate planar devices with low driving E_{bias}, easily integrated with planar circuits. The most popular ferroelectric materials are $Ba_xSr_{1-x}TiO_3$ (BST) [11] and $PbZr_{1-x}Ti_xO_3$ (PZT) [12]. In this work, the attention is focused on an alternative oxide, namely $KTa_{1-x}Nb_xO_3$ (KTN), which exhibits strong potential for tunability [13].

The $KTa_{0.5}Nb_{0.5}O_3$ composition (x = 0.5) is selected here to reach the highest frequency tunability of the device under a moderate biasing (E_{bias} < 100 kV/cm). This composition exhibits a large relative permittivity $\varepsilon_{r(KTN)} \approx 700$, but also leads to significant dielectric loss ($\tan\delta_{r(KTN)} \approx 0.15$–0.30 at 10 GHz) [13,14]. Three main solutions can be considered to overcome this drawback: (i) doping the KTN ferroelectric material in order to lower its intrinsic loss [15]; (ii) confining the KTN film only in specific regions of the device and to remove it in 'non-critical' areas [16]; and (iii) associating the KTN film with a low loss dielectric material to build ferroelectric/dielectric multilayers. The latter solution is investigated here.

The $Bi_{1.5}Zn_{0.9}Nb_{1.5}O_{7-\delta}$ oxide (BZN) has been selected due to its low dielectric loss at microwaves ($\tan\delta_{r(BZN)} \approx 0.005$–0.0075 at 12.5 GHz) [17,18]. It also exhibits a moderate relative permittivity in this frequency band ($\varepsilon_{r(BZN)} \approx 95$–125). For the current study, BZN oxide is used as a pure dielectric material. Nonetheless it can exhibit tunable property, but only under a very high bias field (E_{bias} > 1 MV/cm) [19].

The paper is organized as follows. After a description of the experimental details in Section 2, a numerical study comparing the performance of coplanar waveguide (CPW) stub resonators printed on both heterostructures (KTN/BZN and BZN/KTN) is provided in Section 3. The impact of the BZN thickness and its position in the heterostructures are studied in terms of tunability and global loss. The proposed fabrication process and the experimental results are discussed in Section 4, and the conclusions are drawn in Section 5.

* Corresponding author. Tel.: +33 2 96 60 96 53; fax: +33 2 96 60 96 52.
E-mail address: xavier.castel@univ-rennes1.fr (X. Castel).

0040-6090/$ – see front matter
http://dx.doi.org/10.1016/j.tsf.2013.11.068

2. Experimental details

2.1. Elaboration of KTN and BZN thin films

The $KTa_{0.5}Nb_{0.5}O_3$ and $Bi_{1.5}Zn_{0.9}Nb_{1.5}O_{7-\delta}$ thin films have been deposited in a single run at 700 °C by pulsed laser deposition under an oxygen pressure of 30 Pa on R-plane sapphire substrates (10 mm × 10 mm × 0.5 mm) using a KrF excimer laser ($\lambda = 248$ nm) operating at 2 Hz with a laser fluence of 2 J/cm^2 and a distance of 55 mm between the substrate and the target. Note that a 60%-potassium enriched target (in mol in the form of KNO_3) and a 10%-bismuth + 40%-zinc enriched target (in mol in the form of Bi_2O_3 and ZnO, respectively) were used for the $KTa_{0.5}Nb_{0.5}O_3$ and $Bi_{1.5}Zn_{0.9}Nb_{1.5}O_{7-\delta}$ thin film elaboration respectively, to counterbalance the volatility of the potassium, bismuth and zinc elements during the deposition stages.

2.2. Metallization

Coatings of silver (Ag, 2 μm-thick) and titanium (Ti, 5 nm-thick) were deposited one after another on the oxide films by RF magnetron sputtering technique at room temperature. The titanium film ensures strong adhesion of the silver metallization. The deposition chamber (Plassys MP 450S) contains two sputtering targets (75 mm in diameter): a titanium disk (99.995% purity) and a silver disk (99.999% purity). This configuration makes it possible to deposit the Ag/Ti coating in a complete run without breaking vacuum. During deposition, a RF power of 150 W was supplied to the working target through an automatic matching network. The argon gas pressure (99.9996% purity) into the sputtering chamber was adjusted by a mass flow controller (115 sccm for a total pressure of 1.07 Pa). Sputtering rate has been calibrated for each target (Ag: 146 nm/min, Ti: 19 nm/min). The thickness of each layer is then controlled through the sputtering time.

2.3. Chemical etching

A standard photolithographic wet etching process was used to define the metallic patterns of the stub resonators. After metallization, the samples were spin-coated with a photosensitive resin layer (Microposit S1828 photo resist from Shipley). Then they were exposed to ultraviolet (UV) light through a photomask with the appropriate pattern (Karl Süss MJB3 mask aligner). After developing the exposed photoresist, the Ag and Ti coatings were etched in suitable chemical solutions at room temperature. The silver layer was etched in HNO_3/H_3PO_4/CH_3COOH/H_2O solution with a ratio of 1:4:4:1 (v/v), and the titanium layer in HF/H_2O solution with a ratio of 3:97 (v/v).

2.4. Characterizations, simulations and measurements

X-ray diffraction (XRD) patterns were recorded with a D8 Advanced Brüker AXS (θ–2θ configuration) equipped with a monochromatized Cu Kα_1 radiation source. 2θ angle is swept from 10° to 80° by 0.01° steps. Surface morphology of the oxide films was determined via field-emission scanning electron microscopy (FE-SEM) using a JEOL JSM 6310F system working at a low accelerating voltage (7 kV). The thickness of oxide films was also measured by FE-SEM on cleaved sections.

Numerical simulations were carried out using the finite element method (FEM) implemented in the commercial electromagnetic software ANSYS Ansoft HFSS™.

Measurements at microwaves were performed at room temperature in the frequency range from 1 GHz to 20 GHz using a vector network analyzer (37369A Wiltron) and a probe station after a line–reflect–reflect-match calibration. A maximum bias voltage of 120 V was applied on the device through bias tees (SHF-BT45 HV200) to isolate the vector network analyzer from the DC power supply. The resonance frequency of the CPW stub resonators was controlled by monitoring the external bias voltage. Gold bonding wires (length: 250 μm, diameter: 15 μm) were used to enforce the equipotential condition on both CPW grounds and to prevent the excitation of parasitic slotline modes.

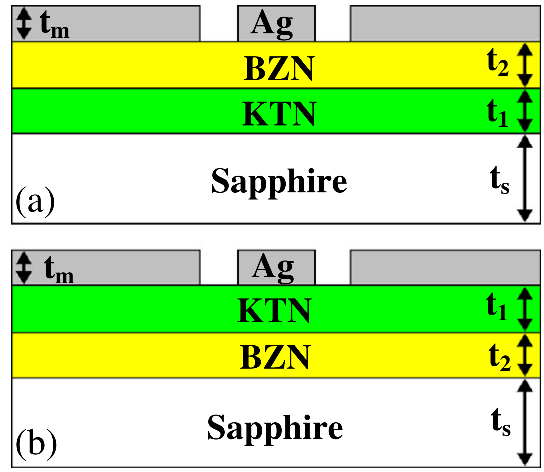

Fig. 1. Cross-sectional view of the coplanar stub resonators: Ag/BZN/KTN/sapphire (a) and Ag/KTN/BZN/sapphire (b).

3. Numerical simulations

Two types of multilayers are compared numerically, namely the BZN/KTN heterostructure and the KTN/BZN one, as shown in Fig. 1. A quarter-wavelength open-ended CPW stub resonator fed by a transmission line (length: 8 mm) is printed on each heterostructure (Figs. 1 and 2). The resonance frequency F_r of the resonator (Eq. (1)) depends on the stub length and the dielectric characteristics of the heterostructure:

$$F_r = \frac{c}{4L_r\sqrt{\varepsilon_{eff}}} \tag{1}$$

where L_r, c and ε_{eff} are the stub length, the speed of light in vacuum, and the effective permittivity of the heterostructure on which the resonator is printed, respectively. The heterostructures are deposited on Al_2O_3 sapphire substrates (relative permittivity $\varepsilon_s = 10$, and loss tangent $\tan\delta_s = 10^{-4}$ at 10 GHz; thickness $t_s = 0.5$ mm). The oxide films are characterized by the following parameters: for KTN: relative permittivity $\varepsilon_{r(\mathrm{KTN})} = 700$ ($E_{bias} = 0$) and 200 (when E_{bias} is applied [14]); loss tangent $\tan\delta_{r(\mathrm{KTN})} = 0.25$ [13]; thickness $t_1 = 600$ nm; and for BZN: $\varepsilon_{r(\mathrm{BZN})} = 100$, $\tan\delta_{r(\mathrm{BZN})} = 10^{-2}$, and its thickness t_2 varies from 0 nm to 600 nm. A silver metallization is used for the coplanar stub resonator (conductivity $\sigma_{Ag} = 6.1 \times 10^7$ S/m [20] and thickness $t_m = 2$ μm). The metallization thickness is three times larger than the skin depth value ($\delta = 0.64$ μm) at the operating frequency (~10 GHz). For simple and efficient numerical simulations, we considered that the relative permittivity of the whole KTN layer is modified under biasing.

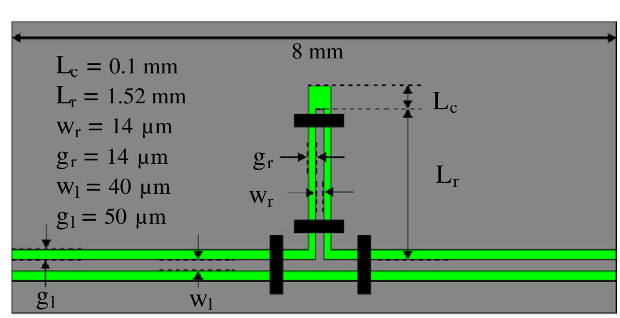

Fig. 2. Layout and dimensions of the coplanar stub resonator (top view). In gray: silver metallization; and in green: oxide multilayer. Black rectangles symbolize gold bonding wires.